Electrical and thermal properties of 10 mol% Gd³⁺ doped ceria electrolytes synthesized through citrate combustion technique

Ramalinga Viswanathan Mangalaraja[1,*], Solaiappan Ananthakumar[2], Manidurai Paulraj[3], Kasimayan Uma[4], Marta López[1], Carlos Porro Camurri[1], Ricardo Enrique Avila[5]

[1]*Department of Materials Engineering, University of Concepción, Concepción, Chile*
[2]*Materials and Minerals Division, National Institute for Interdisciplinary Science and Technology (NIIST), CSIR, Trivandrum, India*
[3]*Department of Physics, University of Concepción, Chile*
[4]*Department of Environmental Technology and Urban Planning, Nagoya Institute of Technology, Nagoya, Japan*
[5]*Department of Nuclear Materials, Chilean Commission of Nuclear Energy, Santiago, Chile*

Abstract

Nanocrystalline ceria electrolyte doped with 10 mol% gadolinia [$Ce_{0.9}Gd_{0.1}O_{1.95}$] was synthesized by citric acid combustion technique involving mixtures of cerium nitrate oxidizer (O) and citric acid fuel (F) taken in the ratio of O/F=1. The as combusted precursors produced crystalline ceria particles upon calcination performed at 700°C for 2h. Ceria pellets were made and sintered at temperatures 1200, 1400 and 1500°C with a dwell time of 2, 4 and 6 h. The sintered microstructures, electrical and thermal conductivities and thermal diffusivity properties were evaluated in addition to the powder properties such as crystalline structure, surface area, particle size and morphology. Sintered ceria samples had 99% theoretical density at 1500°C/6h. The sintered microstructures exhibit dense ceria grains with sizes 500 nm to one micron. The electrical conductivity versus temperature showed conductivity in the order of 10^{-2} and 10^{-1} S·cm⁻¹ at 500 and 700°C, respectively. The ceria sintered at 1500°C has the maximum thermal conductivity of ~2.79 W·m⁻¹K⁻¹ at room temperature.

Keywords: Gadolinia doped ceria, combustion synthesis, electrical conductivity, thermal conductivity

I. Introduction

Development of rare earth doped ceria is a subject of interest because it can replace yttria stabilized zirconia electrolytes for low temperature solid oxide fuel cells (SOFCs). Depending upon the dopants, ceria acts as either oxygen ionic-conductor or ionic-electronic mixed conductor. For the enhancement of ionic conductivity, dopants which have ionic radii very close to ceria are normally selected [1]. Doping with R³⁺ ions (R= Gd, Sm, Nd, Y, Pr, etc.) in the crystal structure of ceria was found to increase the number of extrinsic oxygen vacancies due to the reduction of Ce⁴⁺ to Ce³⁺ that ultimately enhance the bulk ionic conductivity of ceria at the end [2,3]. Gd³⁺ ion doped ceria, particularly 10 mol% Gd³⁺ ion ($Ce_{0.9}Gd_{0.1}O_{1.95}$) is paid more attention because it has been already approved as a potential electrolyte for fuel cells with low operating temperatures [2,4–8]. Since a high dense membrane electrolyte is needed, nanocrystalline Gd³⁺ ion doped ceria powders are being processed. Wet chemical methods have been numerously attempted to synthesize doped ceria nanopowders. Among them, combustion synthesis is treated as one of the promising routes as it can offer reactive powders which can be obtained in one-pot synthesis. It has been found that the evolution of gaseous by-products during combustion limits the inter-particle contacts thus resulting in ultrafine powders [8]. In the present study, we have synthesized gadolinium doped ceria ($Ce_{0.9}Gd_{0.1}O_{1.95}$) by citrate combustion route and assessed its electrical and thermal properties in addition to the powder characteristics. The synthesis of Gd³⁺ ion doped ceria was also attempted earlier through the combustion technique [8,9]. However the extent of particle-agglomeration in presence of various fuels, its dispersion and the effect of particle

* Corresponding author: tel: +56-41 220 7389
fax: +56-41 220 3391, e-mail: *mangal@udec.cl*

size upon densification were the main investigations carried out. Also, most of the studies were devoted to achieve dense ceria at low sintering temperatures. There are available reports available on the electrical conductivity of the gadolinium doped ceria prepared by conventional solid state ceramic route [10], sol-gel [10], precipitation [11], gel-casting [12] and freeze-drying [13] methods. The thermal conductivity and diffusivity data for ceria is seldom reported except the thermal expansion behaviour. The data on electrical and thermal properties of combustion derived doped ceria still has scope for tuning the material for the electrolyte applications.

II. Experimental

2.1 Synthesis

Gadolinium doped ceria was prepared by dissolving cerium nitrate ($Ce(NO_3)_3 \times 6H_2O$, purity 99%) and gadolinium nitrate ($Gd(NO_3)_3 \times 6H_2O$, purity 99.9%) in distilled water. Citric acid (CH_2COOH COH COOH CH_2COOH, purity ≥99.5+%) was used as a fuel. The required amounts of citric acid for complete combustion was calculated using the basic principles of propellant chemistry i.e. the ratio of oxidizing and reducing valencies should be unity [14]. More details on the combustion synthesis are reported in our earlier work [15]. In a typical experiment, for synthesizing one mole of $Ce_{0.9}Gd_{0.1}O_{1.95}$, 0.783 moles of citric acid was taken. A clear homogeneous precursor solution was first prepared in aqueous medium and then transferred into platinum crucible (100 ml). The sample is then subjected to combustion reaction in a preheated electric furnace maintained at 500°C. When the mixture reaches the point of spontaneous combustion, it starts burning and within few minutes porous solid foam (Fig. 1) was obtained. It was collected and crushed for further processing. During combustion reaction, release of dense brown fumes was observed. The release of gases, like NO_2, N_2, CO_2, and H_2O, were expected during the reaction. The as prepared porous $Ce_{0.9}Gd_{0.1}O_{1.95}$ powders were calcined at 700°C for 2h [16].

2.2 Characterization

The as-prepared powders were characterised by thermo-gravimetric analysis at a constant heating rate of 10°C/min in He atmosphere using a Netzsch-STA 409 PC/PG equipped with a mass spectrometer (Balzers MID) for identifying the evolved gases. Crystalline nature and phase purity were examined using powder X-ray diffraction technique (X´Pert Pro, Philips X-ray diffractometer). The X-ray diffraction was recorded using CuK$_\alpha$ radiation. The crystallite size was determined using Scherrer´s equation [17]. Bulk surface area of the as-prepared and calcined powders was measured using Brunauer-Emmett-Teller (BET) method in (Micromeritics ASAP 2010) instrument after properly degassing the powder samples at 100°C. Morphology, particle size and distribution were
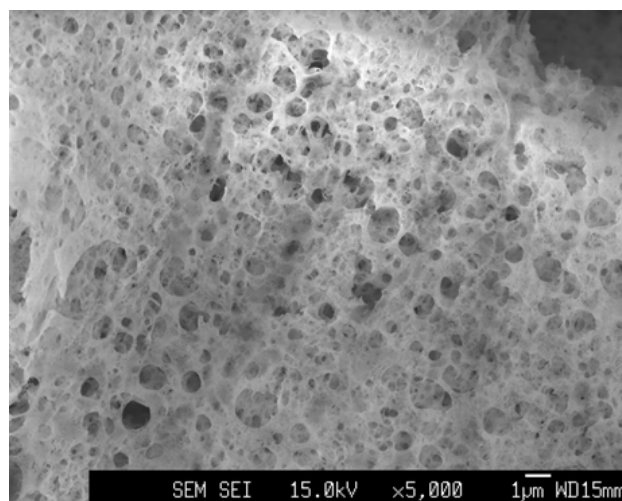
Figure 1. SEM morphology of the as-prepared precursor foam of $Ce_{0.9}Gd_{0.1}O_{1.95}$

analysed by both scanning electron microscope (SEM-JEOL 6460 LV) and transmission electron microscope (TEM-JEOL JEM 2000 EX). TEM samples were prepared by dispersing the powder in dilute ethanol medium under ultrasonic agitation. A drop of suspension was placed on a carbon coated fine mesh copper grid. Once ethanol evaporated, images were captured under TEM.

The powders calcined at 700°C for 2 h were uniaxially pressed into cylindrical pellets and rectangular bars, and sintered at temperatures of 1200, 1400 and 1500°C for 2, 4 and 6 h. The sintered density was measured by Archimedes principle. The DC conductivity of the sintered samples was measured by 4-proble method at temperatures 200 to 1000°C. The room temperature thermal diffusivity (α) values were evaluated by photo-acoustic (PA) technique using a homemade PA cell. In order to determine the thermal diffusivity values, a light beam from a 20 mW He-Ne laser (632.8 nm), modulated using a mechanical chopper (SR 540) was allowed to fall on the sample which was fixed with the PA cell. More experimental details are described elsewhere [18]. The room temperature thermal conductivity, λ (W·m^{-1}·K^{-1}) was calculated using the formula:

$$\lambda = \alpha \cdot \rho \cdot C_p$$

where α is the room temperature thermal diffusivity ($m^2 s^{-1}$), ρ is the sintered density of the sample and C_p is the specific heat capacity (J kg^{-1}K^{-1}). The specific heat capacity of $Ce_{0.9}Gd_{0.1}O_{1.95}$ was calculated using the heat capacity data available in the literature for CeO_2 and Gd_2O_3 oxides. The calculation was followed as per the Neumann-Kopp rule [19]. The Neumann-Kopp rule represents the simplest approach for the estimation of mixed oxide specific heat capacity (C_{pm}) at room temperature (25°C). In this method, the molar heat capacity of the mixed oxide is calculated as a weighted sum of the heat capacities of the constituent oxides.

III. Results and discussion

3.1. TG/DTA

The TG/DT analysis results for the as-prepared and calcined ceria powders are presented in Fig. 2. The as-prepared and calcined $Ce_{0.9}Gd_{0.1}O_{1.95}$ powders showed the total weight loss values as 15 and 10 wt.%, respectively. Both samples showed only single step decomposition and between the two TG curves, a variation in the slope was observed. The as-prepared precursor decomposed comparatively faster than the calcined samples. As expected, the calcined samples showed decreased weight loss. In the as-prepared condition, the precursor has undergone dehydration partly that yield a mixture of semicrystalline and amorphous $Ce(OH)_4 \times H_2O$ in the polymerized citrate gel network. The dehydroxylation followed by densification of ceria nano-clusters caused significant weight loss. In the calcined sample, the weight loss is mainly induced by the removal of structurally bonded water and the un-burnt carbon that remained even after calcination. As seen in earlier studies, the combustion derived Gd^{3+} doped ceria also exhibits weight gain above 1000°C. It may be associated with oxygen uptake due to Ce^{3+} oxidation into Ce^{4+}. This may occur if a part of ceria cations have 3^+ oxidation states after the combustion synthesis. Such behaviour seems quite likely, especially due to the presence of remaining carbon which may reduce ceria cations at the initial stage. The TG curve confirmed a weight gain of 2.3 % for the calcined powders within 1130°C, whereas the as-prepared precursor showed only 0.3 % weight gain even up to 1240°C. In the calcined ceria powders, the ceria crystallites are already formed and they are highly reactive and continue to grow during heating. At temperatures nearly 1130°C, the ceria crystals have grown to its maximum and its crystal lattice started expanding showing increased weight gain. In fact at 700°C, the $Ce_{0.9}Gd_{0.1}O_{1.95}$ powders largely contain crystalline ceria nano-clusters. In the as-prepared precursors, only a porous, amorphous ceria agglomerates are present and during heating the powders undergo dehydroxylation in the initial stage and later crystal growth and densification are simultaneously taking place. Since the densification reaction is associated with the crystal growth, the as-prepared precursors show less weight gain.
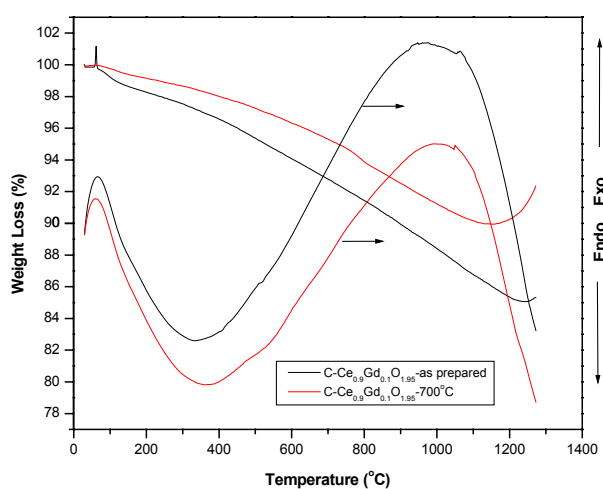
3.2 The role of porous anisotropy

The specific surface areas corresponding to the as-prepared and calcined $Ce_{0.9}Gd_{0.1}O_{1.95}$ powders are 68.1 and 25.7 m^2/g, respectively. A high surface area in the as-prepared powder is an indication of the presence of porous agglomerates and clustering of amorphous nano-particles. The particle-coalescence and crystal growth during calcination significantly decreased the surface area. According to the relation $D = 6000/\rho \cdot S$, where D is the equivalent spherical diameter of the particles (in nm), ρ is the theoretical density of the material (7.159 g/cm^3) and S is the measured specific surface area (in m^2/g), the primary particle sizes of the as-prepared and calcined powders were 12 and 32 nm respectively. It confirms that particles grow considerably during calcination which results in an overall decrease in the intra-particle pore volume. The obtained specific surface area and primary particle size values in our work are found to be better than the earlier values reported for the combustion derived ceria [8].

3.3. X-Ray diffraction

The powder X-ray diffraction analysis of the $Ce_{0.9}Gd_{0.1}O_{1.95}$ powders with and without calcination is shown in Fig. 3. The formation of cubic fluorite ceria is confirmed in both cases. The peaks are matching well with the cerium oxide JCPDS card No: 34-394. All the peaks can be assigned to the crystal planes (111) (200) (220) (311) (222) (400) (331) and (420). There are no peaks detected for the gadolinium oxide. It indicates that the dopant ion is fully substituted in the CeO_2 lattice.

Figure 2. Thermal analysis of as-prepared and calcined powders of $Ce_{0.9}Gd_{0.1}O_{1.95}$
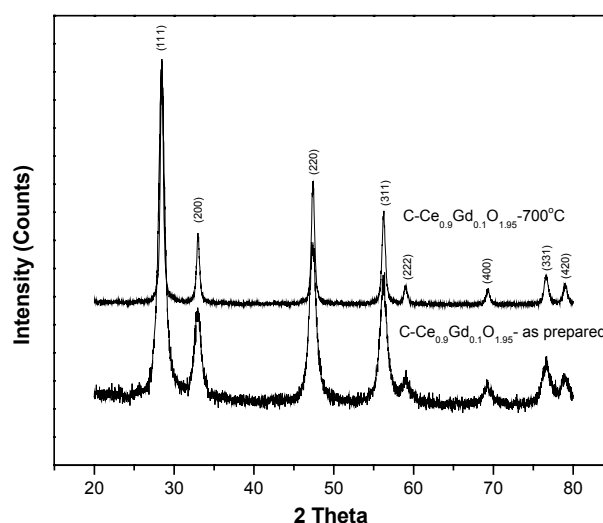
Figure 3. X-ray diffraction pattern of the $Ce_{0.9}Gd_{0.1}O_{1.95}$ powders derived using citric acid and calcined at 700°C
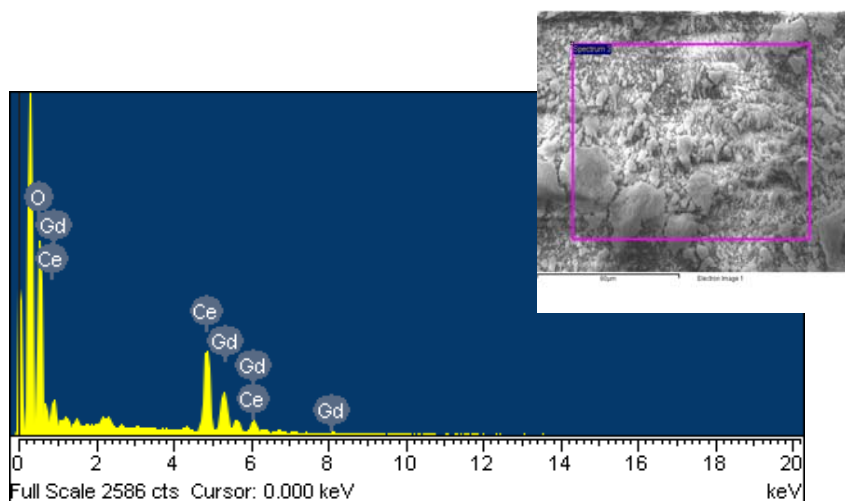
Figure 4. Chemical analysis spectrum of EDS attached with SEM for calcined $Ce_{0.9}Gd_{0.1}O_{1.95}$ powder

Since the XRD shows only fluorite type structure we can believe that only 'true fluorite cubic solid-solution' is formed. In the as-prepared precursors the peaks have wider width indicating that the crystallites are smaller. The primary crystallite size values calculated from the X-ray broadening data were found to be 5 and 14 nm for the as-prepared and calcined powders, respectively. The difference between these values is due to the heating effect. Though these values are of an order smaller compared to the particle sizes calculated from the surface area data, the order of crystallite size increase between the as-prepared and calcined samples is similar to the values obtained from the surface area data.

3.4 Powder Morphology

SEM image of the as-prepared $Ce_{0.9}Gd_{0.1}O_{1.95}$ powder is presented in Fig. 4, showing its porous and spongy nature. Formations of extremely small particles are clearly seen. However, the SEM also showed the presence of agglomerates in a localized manner. During combustion, the metal nitrates are impregnated into the citrate gel polymeric-network. During ignition, the heat dissipation and the evolution of gaseous products are taking place at various rates which ultimately leads to a localized heating and formation of large agglomerates. The porous nature is formed out of the fast expulsion of the gases. The chemical compositions can be clearly identified by the EDS analysis spectrum, which is also shown as an insert along with the SEM image. It confirms that the chemical composition is only $Ce_{0.9}Gd_{0.1}O_{1.95}$ and the powder has no other impurities. TEM micrographs corresponding to the calcined $Ce_{0.9}Gd_{0.1}O_{1.95}$ are presented in Fig. 5. The TEM image shows that the particles are composed of individual crystals and they are slightly elongated in the shape. It shows an average length of 25 nm and the width of 5 nm.

3.5 Sintering and Microstructures

The densities of the $Ce_{0.9}Gd_{0.1}O_{1.95}$ pellets sintered at temperatures 1200, 1400 and 1500°C with various dwell times are shown in Fig. 6. It is observed that the $Ce_{0.9}Gd_{0.1}O_{1.95}$ pellets could be sintered near to its theoretical value at low temperatures provided a prolonged heating. In this study, the sample heated for 6 h at 1200°C has 90% of theoretical density (TD). The sintered density is gradually increasing with respect to the
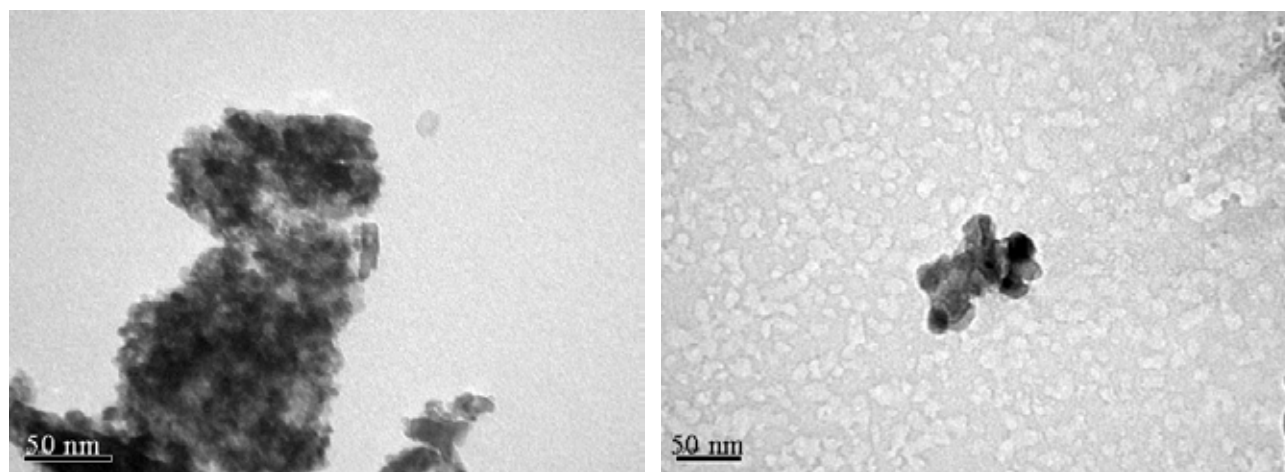
Figure 5. TEM photographs of calcined $Ce_{0.9}Gd_{0.1}O_{1.95}$ powder
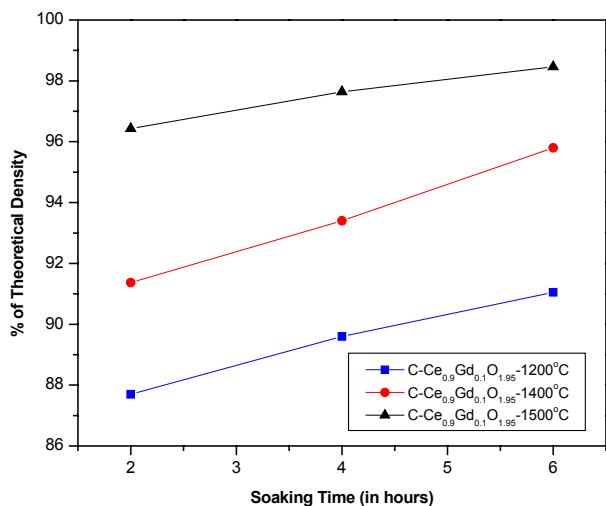
Figure 6. Sintered density variation with respect to dwell time

given sintering temperatures and dwell time. Heating at 1400°C for 6 h resulted in sintered density of 96 %TD. Nearly 99 %TD was obtained for the samples sintered at 1500°C for 6 h. The densities of $Ce_{0.9}Gd_{0.1}O_{1.95}$ samples sintered at 1500°C for 2, 4 and 6 h were 96.5, 97.7 and 98.5 %TD respectively. These values are comparatively higher than those of the reported results [5,12]. This indicates that the $Ce_{0.9}Gd_{0.1}O_{1.95}$ powders prepared by the combustion technique have enhanced sinterability. The sintering temperature of 1500 to 1550°C is usually employed and such high temperature range required due to the fact that dense ceria is a primary requirement for the electrolyte application.

The SEM micrographs of the as-sintered surface of $Ce_{0.9}Gd_{0.1}O_{1.95}$ pellets and their fractured surface are shown in Fig. 7a,b. These images are corresponding to the sintering temperature of 1500°C with dwell time of 6 h. Both micrographs clearly show that the grains are denser and the microstructure has no porosity except the presence of few grain-pull outs. There are also no intragranular pores. From the SEM micrographs, we can see that the sintered $Ce_{0.9}Gd_{0.1}O_{1.95}$ pellets have the grain size variations between 500 nm to 1.0 μm even at 1500°C for 6 h. It also showed the presence of smaller grains in the order of <300 nm. The chemical composition of the sintered samples observed by EDS attached with the SEM is also shown in Fig. 8 for further references.
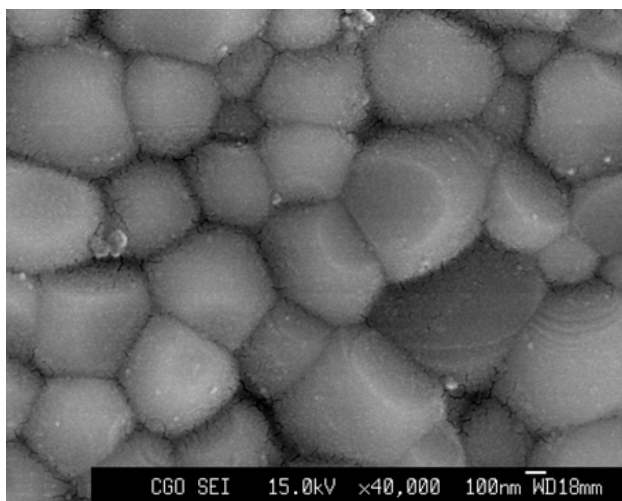
a)
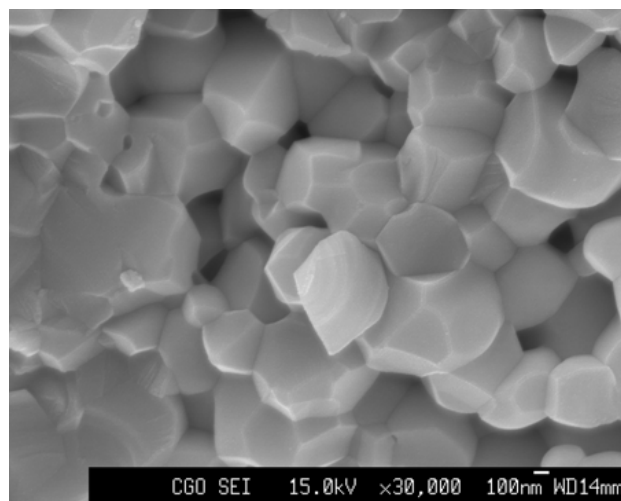
b)

Figure 7. SEM micrographs of $Ce_{0.9}Gd_{0.1}O_{1.95}$ sintered at 1500°C for 6 h (a) as-sintered surface and (b) fractured surface
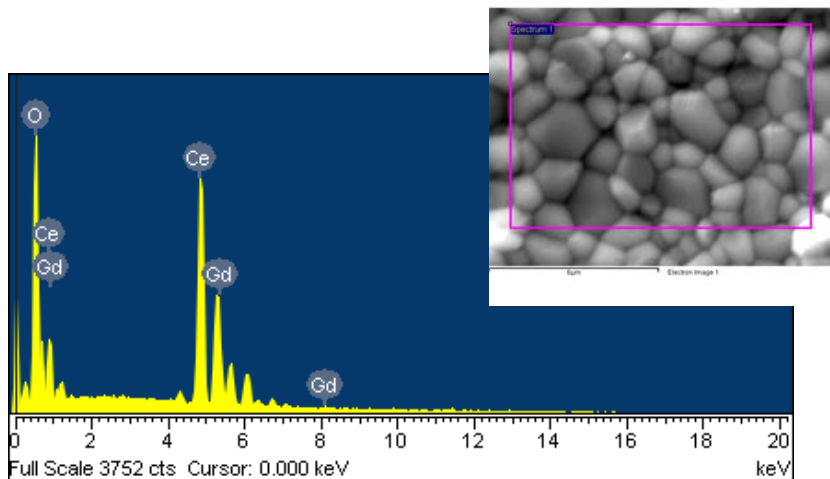
Figure 8. Chemical analysis spectrum of EDS attached with SEM for sintered $Ce_{0.9}Gd_{0.1}O_{1.95}$

Table 1 Thermal diffusivity and conductivity of sintered $Ce_{0.9}Gd_{0.1}O_{1.95}$

Sintering temperature* [°C]	Sintered density [g·cm⁻³]	Thermal diffusivity [10^{-6} m²·s⁻¹]	Thermal conductivity [W·m⁻¹K⁻¹]
1200	6.56±0.7	0.57±0.8	1.31
1400	6.89±0.05	1.04±0.5	2.52
1500	7.09±0.05	1.12±0.4	2.79

*Sintering with 6 h dwell time

3.6 Electrical Conductivity

The electrical conductivities of the sintered $Ce_{0.9}Gd_{0.1}O_{1.95}$ samples fabricated in this study and sintered at 1400 and 1500°C for 2, 4 and 6 h are shown Fig. 9. In earlier studies the electrical conductivity of ceria is correlated with the sintering temperature, sintered microstructure, oxygen partial pressure in the surrounding gas atmosphere, the type and concentration of the dopants [20–22]. The reports also showed that the dopants are highly important to achieve increased grain conductivity. Typically impedance spectroscopy data is required to prove the grain conductivity and grain boundary resistance. In our study we could not collect any such data due to lack of facility. However, there are reports on the dependence of the Gd-ion doping on the ceria conductivity and they say that due to high solubility limit of Gd-ions in ceria, the total conductivity i.e the grain boundary and bulk conductivity, is increased. We have studied the temperature dependence of the electrical conductivity (σ) of $Ce_{0.9}Gd_{0.1}O_{1.95}$ samples and drawn the Arrhenius plot (Fig. 9). Between the sintering temperatures of 1400 and 1500°C, due to the increased sintered density, the $Ce_{0.9}Gd_{0.1}O_{1.95}$ samples sintered at 1500°C showed a higher conductivity. The electrical conductivities of 0.03 and 0.049 S·cm⁻¹ at 600 and 700°C, respectively were obtained for the samples sintered at 1500°C for 6 h. The electrical conductivity values are still high at 975°C (0.15 and 0.19 S·cm⁻¹) for both samples sintered at temperatures 1400 and 1500°C for 6 h.
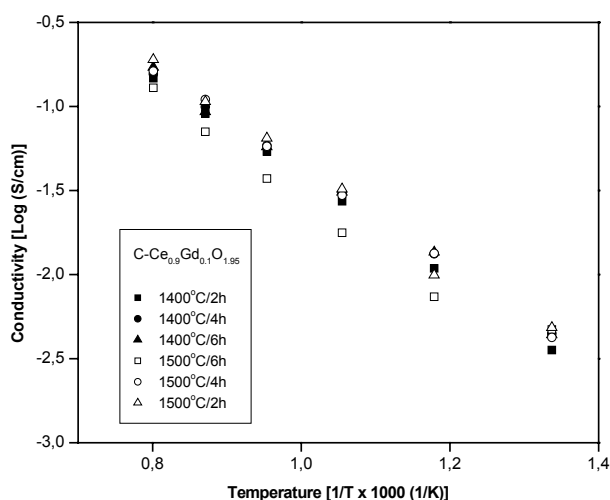
Figure 9. Variation of DC-electrical conductivity with respect to temperature for samples sintered at 1400 and 1500°C for different dwell time

The increased electrical conductivity may be due to the low grain size, the homogeneous distribution of Gd^{3+} in ceria lattice and its high ionic-mobility. The ionic conductivity values obtained in our work are higher than those of the values reported earlier [5,12,20].

3.7 Thermal Conductivity

The room temperature (25°C) thermal diffusivity values evaluated by photo-acoustic technique [18] and the thermal conductivities calculated for $Ce_{0.9}Gd_{0.1}O_{1.95}$ samples sintered at 1200, 1400 and 1500°C for 6 h are presented in the Table 1. Studies concerning the thermal expansion of doped ceria were widely attempted rather than the thermal conductivity. In fact ceria is a preferred top coat in thermal barrier coatings only due to its low thermal conductivity. However, the thermal conductivity of the sintered oxide ceramics strongly depends on the microstructural features such as surface finish, grain size, and porosity of the sintered material. Here, we obtained a low thermal conductivity only for the samples sintered at 1200°C which is actually the effect of the porosity present in the material. The thermal diffusivity and conductivity values are showing increasing trend with respect to the sintering temperatures. Though the enhanced densification at high sintering temperatures is a reason for high thermal diffusivity and thermal conductivity, obviously the grain size plays a key role. The thermal conductivity of the gadolinium doped ceria thin films have been earlier reported by Muthukumaran et al [23]. Burghartz et al [24] have reported thermal diffusivity and thermal conductivity of pure ceria to be 1.96×10^{-6} m²s⁻¹ and 5.117 W·m⁻¹K⁻¹, respectively at 600 K. With regard to nanostructured ceria thin films, the nanograins resulted in low thermal conductivities if the microstructure consisting grains below 50 nm in size. In nanocrystalline solids the thermal conduction is governed by the structural defects present in the crystallites. Once the average grain size is nearly a micron, the grain boundary phonon scattering is the active phenomena for the thermal conduction. In our case, the grain size increase with respect to the sintering temperature caused significant increase in the thermal conductivity.

IV. Conclusions

$Ce_{0.9}Gd_{0.1}O_{1.95}$ nanocrystalline powders were prepared by citrate gel-combustion. The specific surface area of the as-prepared ceria powder was 68.1 m²/g

and decreased after calcination to 25.7 m²/g. The powder particles had shown elongated nanocrystalline ceria particles with crystallite size in the range of 5 to 20 nm. A density of 99 %TD was achieved at the sintering temperature of 1500°C for 6 h. The sintered microstructure showed dense ceria grains with the grain size in the order of 500 nm to one micron. The electrical conductivity was assessed for the combustion derived doped $Ce_{0.9}Gd_{0.1}O_{1.95}$ and we noted that it was 0.03 and 0.049 S·cm⁻¹ at 600 and 700°C, respectively for the samples sintered at 1500°C for 6 h. The high density, small grain size and the dopant ion mobility were the probable reasons for increased conductivity. The room temperature thermal diffusivity and the thermal conductivity values were seen as 1.12×10^{-6} m²s⁻¹ and 2.79 W·m⁻¹K⁻¹ for the sintered $Ce_{0.9}Gd_{0.1}O_{1.95}$ at 1500°C for 6 h.

References

1. T. Suzuki, I. Kosacki, H.U. Anderson, "Defect and mixed conductivity in nanocrystalline doped cerium oxide", *J. Am. Ceram. Soc.*, **85** (2002) 1492–1498.
2. V. Esposito, E. Traversa, "Design of electroceramics for solid oxide fuel cells applications: Playing with ceria", *J. Am. Ceram. Soc.*, **91** [4] (2008) 1037–1051.
3. M.-Y. Cheng, D.-H. Hwang, H.-S. Sheu, B.-J. Hwang, "Formation of $Ce_{0.8}Sm_{0.2}O_{1.9}$ nanoparticles by urea based low-temperature hydrothermal process", *J. Power Sources*, **175** (2008) 137–144.
4. B.C.H. Steele, "Appraisal of $Ce_{1-y}Gd_yO_{2-y/2}$ electrolytes for IT-SOFC operation at 500°C", *Solid State Ionics*, **129** (2000) 95–110.
5. J. Cheng, S. Zha, X. Fang, X. Lin, G. Meng, "On the green density, sintering behaviour and electrical property of tape cast $Ce_{0.9}Gd_{0.1}O_{1.95}$ electrolyte films", *Mater. Res. Bull.*, **37** (2002) 2437–2446.
6. M. Mogensen, N.M. Sammes, G.A. Tompsett, "Physical, chemical and electrochemical properties of pure and doped ceria", *Solid State Ionics*, **129** (2000) 63–64.
7. C. Xia, M. Liu, "Low-temperature SOFCs based on $Ce_{0.9}Gd_{0.1}O_{1.95}$ fabricated by dry pressing", *Solid State Ionics*, **144** (2001) 249–255.
8. T. Mahata, G. Das, R.K. Mishra, B.P. Sharma, "Combustion synthesis of gadolinia doped ceria", *J. Alloys Comp.*, **391** (2005) 129–135.
9. W. Chen, F. Li, J. Yu, "Combustion synthesis and characterization of nanocrystalline CeO_2 – based powders via ethylene glycol-nitrate process", *Mater. Lett.*, **60** (2006) 57–62.
10. K. Huang, J.B. Goodenough, "Synthesis and electrical properties of dense $Ce_{0.9}Gd_{0.1}O_{1.95}$ ceramics", *J. Am. Ceram. Soc.*, **81** [2] (1998) 357–362.
11. A. Sin, Yu. Dubitsky, A. Zaopo, A.S. Arico, L. Gullo, D. La Rosa, S. Siracusano, V. Antonucci, C. Oliva, O. Ballabio, "Preparation and sintering of $Ce_{1-x}Gd_xO_{2-x/2}$ nanopowders and their electrochemical EPR characterization", *Solid State Ionics,* **175** (2004) 361–366.
12. J-G. Cheng, S-W. Zha, J. Huang, X-Q. Liu, G-Y. Meng, "Sintering behaviour and electrical conductivity of $Ce_{0.9}Gd_{0.1}O_{1.95}$ powder prepared by gel-casting process", *Mater. Chem. Phys.*, **78** (2003) 791–795.
13. D. Perez-Coll, P. Nunez, J.R. Frade, J.C.C. Abrantes, "Conductivity of CGO and CSO ceramics obtained from freeze-dried precursors", *Electrochim. Acta*, **48** (2003) 1551–1557.
14. S. Ekambaram, K.C. Patil, "Combustion synthesis of yttria", *J. Mater. Chem.*, **5** [6] (1995) 905–908.
15. R.V. Mangalaraja, J. Mouzon, P. Hedström, I. Kero, K.V.S. Ramam, C.P. Camurri, M. Odén, "Combustion synthesis of Y_2O_3 and Yb- Y_2O_3: Part I - Nanopowders and its characterization", *J. Mater. Proc. Tech.*, **208** [1-3] (2008) 415–422.
16. T.S. Zhang, J. Ma, L.B. Kong, P. Hing, J.A. Kilner, "Preparation and mechanical properties of dense $Ce_{0.8}Gd_{0.2}O_{2-\delta}$ ceramics", *Solid State Ionics*, **167** (2004) 191–196.
17. B.D. Cullity, "Elements of X-ray diffraction", Second Edition., Addison-Wesley, MA, 1978.
18. K. Raveendranath, J. Ravi, R.M. Tomy, S. Jayalekshmi, R.V. Mangalaraja, S.T. Lee, "Evidence of Jahn-Teller distortion in $Li_xMn_2O_4$ by thermal diffusivity measurements", *Appl. Phys.* A **90** (2008) 437–440.
19. J. Leitner, P. Chuchvalec, D. Sedmidubsky, A. Strejc, P. Abrman, "Estimation of heat capacities of solid mixed oxides", *Thermochim. Acta*, **395** (2003) 27–46.
20. X.D. Zhou, W. Huebner, I. Kosacki, H.U. Anderson, "Microstructure and grainboundary effect on electrical properties of gadolinia-doped ceria", *J. Am. Ceram. Soc.*, **85** (2002) 1757–1762.
21. S. Hui, J. Roller, S. Yick, X. Zhang, C.D. Petit, Y. Xie, R. Maric, D. Ghosh, "A brief review of the ionic conductivity enhancement for selected oxide electrolytes", *J. Power Sources*, **172** (2007) 493–502.
22. H. Inaba, H. Tagawa, "Ceria based solid electrolytes", *Solid State Ionics*, **83** (1996) 1–16.
23. K. Muthukumaran, P. Kuppusami, R. Srinivasan, K. Ramachandran, E. Mohandas, S. Selladurai, "Thermal properties of 15-mol% gadolinia doped ceria thin films prepared by pulsed laser ablation", *Ionics*, **13** (2007) 47–50
24. M. Burghartz, Hj. Matzke, C. Léger, G. Vambenepe, M. Rome, "Inert matrices for the transmutation of actinides: fabrication, thermal properties and radiation stability of ceramic materials", *J. Alloys Comp.*, **271-273** (1998) 544–548.